

YidC1 and YidC2 are functionally distinct proteins involved in protein secretion, biofilm formation and cariogenicity of *Streptococcus mutans*

Sara R. Palmer,¹ Paula J. Crowley,¹ Monika W. Oli,¹ M. Adam Ruefl,¹ Suzanne M. Michalek² and L. Jeannine Brady¹

Correspondence

L. Jeannine Brady

jbrady@dental.ufl.edu

¹Department of Oral Biology, University of Florida, PO Box 100424, Gainesville, FL 32610-0424, USA

²Department of Microbiology, University of Alabama at Birmingham, Birmingham, AL 35294-2170, USA

The cariogenic bacterium *Streptococcus mutans* has two paralogues of the YidC/Oxa1/Alb3 family of membrane protein insertases/chaperones. Disruption of *yidC2* results in loss of genetic competence, decreased membrane-associated ATPase activity and stress sensitivity (acid, osmotic and oxidative). Elimination of *yidC1* has less severe effects, with little observable effect on growth or stress sensitivity. To examine the respective roles of YidC1 and YidC2, a conditional expression system was developed allowing simultaneous elimination of both endogenous YidCs. The function of the YidC C-terminal tails was also investigated and a chimeric YidC1 protein appended with the C terminus of YidC2 enabled YidC1 to complement a $\Delta yidC2$ mutant for stress tolerance, ATP hydrolysis activity and extracellular glyceraldehyde-3-phosphate dehydrogenase (GAPDH) activity. Elimination of *yidC1* or *yidC2* affected levels of extracellular proteins, including GtfB, GtfC and adhesin P1 (Agl/II, PAc), which were increased without YidC1 but decreased in the absence of YidC2. Both *yidC1* and *yidC2* were shown to contribute to *S. mutans* biofilm formation and to cariogenicity in a rat model. Collectively, these results provide evidence that YidC1 and YidC2 contribute to cell surface biogenesis and protein secretion in *S. mutans* and that differences in stress sensitivity between the $\Delta yidC1$ and $\Delta yidC2$ mutants stem from a functional difference in the C-termini of these two proteins.

Received 7 March 2012

Revised 6 April 2012

Accepted 11 April 2012

INTRODUCTION

Acidogenic and acidophilic bacteria within the supragingival plaque on teeth are responsible for dental caries. *Streptococcus mutans* is highly acidogenic and mounts an acid tolerance response to cope with the acid produced, thus enabling it to outcompete other bacteria in the oral cavity (Hamilton & Buckley, 1991). An avid biofilm former, *S. mutans* adheres to the tooth surface through sucrose-dependent [glucosyltransferases (GTFs) and fructosyltransferases (FTFs)] and sucrose-independent (antigen I/II, aka P1 or PAc) mechanisms (Gibbons *et al.*, 1986; Jenkinson & Lamont, 1997). During a search for *S. mutans* genes that contribute to acid tolerance, a mutant disrupted in *ffh* expression was isolated (Gutierrez *et al.*, 1996). The *ffh* gene encodes an integral component of the signal

recognition particle (SRP) co-translational targeting pathway, which was previously believed to be essential for viability in all cells, including bacteria (Honda *et al.*, 1993; Phillips & Silhavy, 1992). Subsequent analysis of the *S. mutans* genome revealed genes encoding two paralogues of the YidC/Oxa1/Alb3 family, YidC1 and YidC2, that appear to supplement the SRP pathway in this organism (Funes *et al.*, 2009). This family of proteins is universally conserved in all three domains of life (Zhang *et al.*, 2009): Oxa1 is in the inner mitochondrial membrane; YidC is in the bacterial cytoplasmic membrane; and Alb3 is in the thylakoid membrane of chloroplasts. These proteins serve as membrane-integral chaperones and insertases with conserved functions in the insertion of respiratory chain complexes, F₁F₀ ATP synthase components and light-harvesting chlorophyll-binding proteins (Bonney *et al.*, 2009; Kiefer & Kuhn, 2007; van der Laan *et al.*, 2003). In mitochondria, chloroplasts and most Gram-positive bacteria, there are often two or more paralogues, whereas *Escherichia coli* and other Gram-negative bacteria have only one.

Abbreviations: SOE, splice overlap extension; SRP, signal recognition particle.

Three supplementary tables, two supplementary figures and a set of supplementary methods are available with the online version of this paper.

Elimination of *yidC2* in *S. mutans* results in a stress-sensitive phenotype similar to *S. mutans* SRP pathway mutants, including growth impairment under acid, osmotic and oxidative stress conditions, decreased membrane-associated ATPase activity, decreased genetic competence and impaired biofilm formation (Hasona *et al.*, 2005). Disruption of *yidC1* has a much less severe effect, with no obvious growth defects or stress sensitivity. YidC2, but not YidC1, can complement a yeast Oxal mutant for growth on a non-fermentable carbon source (Funes *et al.*, 2009). This ability requires the C terminus of YidC2. In contrast, either YidC1 or YidC2 can complement an *E. coli* YidC depletion strain for growth and restore functional activity to the F₁F₀ ATP synthase (Dong *et al.*, 2008). Previous attempts to isolate double mutants in the SRP pathway and *yidC2* have been unsuccessful. It has also not been possible to simultaneously eliminate *yidC1* and *yidC2*, suggesting overlapping functions in the SRP and YidC2 pathways, as well as between YidC1 and YidC2.

The work presented here highlights the complex nature of protein translocation and maturation in *S. mutans* and supports the hypothesis that pathway redundancies allow the organism to thrive under environmentally stressful conditions, establish biofilms and cause disease. We developed a conditional expression system for *yidC2* to

enable the simultaneous elimination of endogenous YidC1 and YidC2. In addition, C-terminal-domain substitutions between YidC1 and YidC2 indicated that the C terminus of YidC2 is critical for the ability of *S. mutans* to tolerate environmental stress. Our studies show further that both YidC1 and YidC2 contribute to *S. mutans* protein secretion, cell surface biogenesis, biofilm formation and cariogenicity, albeit in different ways and to different extents.

METHODS

Bacterial strains, plasmids and growth conditions. Table 1 lists strains and plasmids, and Table S1 (available with the online version of this paper) lists primers used in this study. A schematic representation of the strains used in this study is shown in Fig. S1. *S. mutans* strains were routinely grown at 37 °C in Todd-Hewitt broth (BBL, Becton Dickinson) supplemented with 0.3% yeast extract (THYE) or in FMC (Terleckyj *et al.*, 1975), modified as described in the Supplementary Methods [Terleckyj's defined medium (TDM)], with 0.5% (w/v) sugar when indicated. Spectinomycin (1 mg ml⁻¹), kanamycin (500 µg ml⁻¹) or erythromycin (5 µg ml⁻¹) were added where appropriate. *E. coli* strain Top10 (Invitrogen), used for intermediate cloning steps, was grown aerobically at 37 °C in Luria-Bertani (LB) broth or agar with kanamycin (50 µg ml⁻¹), spectinomycin (100 µg ml⁻¹) or erythromycin (150 µg ml⁻¹) where appropriate.

Table 1. Bacterial strains and plasmids used in this study

em, Erythromycin; km, kanamycin; ap, ampicillin; sp, spectinomycin; tc, tetracycline; MCS, multiple cloning site.

Strain/plasmid	Relevant characteristic(s)	Source
<i>S. mutans</i>		
UA159	Wild-type	R. A. Burne
NG8	Wild-type	Knox <i>et al.</i> (1986)
PC3370	NG8 $\Delta spaP::tc$	Crowley <i>et al.</i> (1999)
AH398	NG8 $\Delta yidC2::em$	Hasona <i>et al.</i> (2005)
AH378	NG8 $\Delta yidC2::km$	A. Hasona
AH374	NG8 $\Delta yidC1::em$	Hasona <i>et al.</i> (2005)
AH412	NG8 $yidC2\Delta C^{255-310}::em$	Funes <i>et al.</i> (2009)
SP10	AH398 $gtfA::P_{celB}-yidC2-km$	This study
SP13	AH378 $gtfA::P_{gtfA}::yidC1^{1-249}-yidC2^{246-310}-em$	This study
SP14	AH378 $gtfA::P_{gtfA}::yidC2^{1-247}-yidC1^{228-271}-em$	This study
SP16	AH412 $\Delta yidC1::sp$	This study
SP17	AH378 $gtfA::P_{gtfA}-yidC2-em$	This study
SP20	SP10 $\Delta yidC1::sp$	This study
SP22	NG8 $gtfA::em$	This study
Plasmids		
pDL289	<i>E. coli</i> - <i>Streptococcus</i> shuttle vector; Km ^r (<i>aphA</i>)	Buckley <i>et al.</i> (1995)
pDL278	<i>E. coli</i> - <i>Streptococcus</i> shuttle vector, Sp ^r (<i>aad9</i>)	LeBlanc <i>et al.</i> (1992)
pBGK2	<i>Streptococcus</i> integration vector at the <i>gtfA</i> locus (same as pBGK with <i>bla</i> deleted)	Wen & Burne (2001)
pBGE	<i>Streptococcus</i> integration vector, genes are expressed from the <i>gtfA</i> promoter in the chromosome	Zeng & Burne (2009)
pSP10	pBGK2 with <i>P_{celA}-yidC2</i> cloned into <i>SmaI</i> site	This study
pSP11	pBGK2 with <i>P_{celB}-yidC2</i> cloned into <i>SmaI</i> site	This study
pCR2.1	T/A cloning vector, <i>LacZx</i> MCS, Ap ^r , Km ^r	Invitrogen
pCR2.1- $\Delta yidC1Sp^R$	pCR2.1 with $\Delta yidC1::sp$ for allelic replacement of <i>yidC1</i>	This study

Strain construction

YidC2 conditional expression strains. UA159 genomic DNA was used as the template in PCRs unless otherwise indicated. The *celB* promoter (*P_{celB}*; -1 to -263) was amplified by PCR using primers SP13F and SP13R. The *yidC2* gene was amplified by PCR using primers SP14F and SP05R. Each PCR product was ligated to pCR2.1, and a 1 kb fragment from a properly oriented *yidC2*-containing-plasmid, cut with *Bam*HI and *Nde*I, was ligated to a 5.0 kb fragment containing *P_{celB}* to create the promoter fusion *P_{celB}-yidC2*. The *P_{celB}-yidC2* fragment was excised with *Sma*I and ligated to *Sma*I-digested pBGK2. The resulting plasmid, pSP10, was used to transform a *S. mutans* $\Delta yidC2$ mutant strain, AH398, resulting in strain SP10 in which *P_{celB}-yidC2* had integrated into the chromosome at the *gtfA* locus (illustrated in Fig. S1). Strain SP10 was confirmed by PCR using primers SP17F and SP16R. Primers SP17F-RC and SP18R were used to confirm orientation of the insert in the *gtfA* locus. Strain SP10 was used to create strain SP20, where *yidC1* was deleted using pCR2.1 $\Delta yidC1::Spec^R$ (see below).

YidC1 deletion strain. *yidC1* was eliminated by allelic replacement with a spectinomycin-resistance (*spec*) gene cassette constructed as follows: splice overlap extension (SOE) PCR (Heckman & Pease, 2007) was used to combine PCR-amplified fragments upstream and downstream of *yidC1* with an intervening *spec* gene amplified from pDL278. Primer pairs used were SP29F and SP24RSOE, SP25FSOE and SP25RSOE, and SP26FSOE and AH25R, respectively. Primers SP29F and SP25RSOE were used to combine the *yidC1* upstream and *spec* fragments by SOE PCR. This product was combined with the *yidC1* downstream fragment by SOE PCR using primers SP29F and AH25R to generate a 2087 nt product that was subsequently ligated to pCR2.1, generating plasmid pCR2.1 $\Delta yidC1Sp^R$. This plasmid was linearized with *Hind*III and used to naturally transform *S. mutans* resulting in replacement of the *yidC1* gene with the spectinomycin-resistance gene via double-crossover recombination.

Construction of genes encoding chimeric YidC1–YidC2 proteins. SOE PCR was used to create a chimeric gene encoding a protein composed of amino acids 1–229 of YidC1 and the C-terminal tail of YidC2 (amino acids 247–310). The *yidC1* fragment (-131 to +687) was amplified by PCR using primers SP21F and SP22RSOE. The *yidC2* C-terminal gene fragment (+741 to +1009) was amplified by PCR using primers SP22FSOE and SP21R. Each fragment was gel-purified and combined via SOE PCR, using primers SP21F and SP21R. The product was ligated to pCR2.1, excised with *Xba*I and *Bsr*GI and ligated to integration vector pBGE that had been similarly digested. Plasmid pBGE-*yidC1-C2-Erm* was used to transform AH378 to generate strain SP13 (see Figs S1 and S2).

A chimeric protein comprising amino acids 1–247 of YidC2 and C-terminal amino acids 227–271 of YidC1 was constructed in the same manner as described above. The *yidC2* gene fragment (-43 to +741) was amplified by PCR with primers SP27F2 and SP27RSOE. The *yidC1* C-terminal fragment (+685 to +875) was amplified by PCR using primers SP28FSOE and SP28R. Fragments were used as templates in an SOE PCR with primers SP27F2 and SP28R. The amplified product was ligated to pCR2.1, excised and ligated to pBGE, and the *Xba*I site in pCR2.1 was used to restrict the fragment from the plasmid for subcloning. The resultant strain was named SP14. The control strain SP17, where unaltered *yidC2* was amplified by PCR using primers SP27F2 and SP21R and placed under control of the *gtfA* promoter in strain NG8, was generated for experiments with SP13 and SP14. The control strain SP22 was created by transforming strain NG8 with pBGE. Proper integration of chimeric and control genes was verified by PCR using the *PgtfA*-based forward primer SP37F and reverse primer AH31R for strains SP13 and SP17, or SP21R for SP14, followed by DNA sequencing.

YidC2 depletion conditions. To determine the conditions necessary to deplete YidC2 in strains SP20 and SP10, cells were grown for 16 h in TDM broth with 0.5% cellobiose then diluted 1:20 into fresh TDM cellobiose (inducing sugar) or TDM-glucose, -fructose or -mannose (repressing sugars). Cultures were grown to OD₆₀₀ 0.9 and diluted in an equal volume of fresh TDM containing the same sugar with continued incubation. This was repeated three times or until growth slowed, indicating depletion of YidC2. Growth in TDM-mannose was the only condition that resulted in reduced growth and depletion of YidC2 occurred after an additional 8 h of growth, as determined by Western blot analysis of cell lysates.

For evaluation of growth on agar, cells were grown 16 h in TDM-cellobiose and diluted 1:10 into fresh TDM-cellobiose and grown to mid-exponential phase. They were then streaked on TDM agar containing 0.5% cellobiose or 0.5% mannose and incubated at 37 °C in a 5% CO₂ incubator for 48 h.

Western blot analysis. To determine depletion conditions of YidC1 and YidC2 in SP20 and SP10, cells from a mid-exponential-phase culture (OD₆₀₀ 0.5) were pelleted and washed once in 25 mM Tris/HCl, pH 7.5 and then resuspended in 500 μ l of the same buffer. Cells were lysed with glass beads (0.1 mm, 0.5 g, BioSpec Products) in a Mini Bead Beater (BioSpec Products), for two 1 min cycles with cooling on ice in between. Proteins were separated by SDS-PAGE through a 10% gel followed by transfer to an Immobilon PVDF membrane (GE Healthcare). Western blots were performed using the ECL kit (GE Healthcare) according to the manufacturer's instructions. Membranes were reacted with affinity-purified YidC1 C-terminal or YidC2 C-terminal antibodies (Dong *et al.*, 2008) at 1:4000 and 1:8000 dilutions, respectively.

For detection of extracellular Gtf B and C, proteins in 500 μ l filter-sterilized supernatant (0.2 μ m filter) from 16 h THYE cultures were precipitated with an equal volume of 20% (v/v) TCA on ice for 20 min. Pellets were washed twice with 300 μ l acetone, resuspended in 100 μ l 50 mM Tris-HCl (pH 7.5) containing 10 mM EDTA. Protein samples were separated by SDS-PAGE through a 4–15% gradient mini gel (Bio-Rad). Western blot analysis was performed as described above using a polyclonal rabbit antiserum (1:500), kindly provided by Dr William Bowen, University of Rochester, that recognizes both GtfB and GtfC (Wunder & Bowen, 2000).

Evaluation of bacterial growth. Cultures of *S. mutans* strains grown for 16 h were diluted 1:20 in THYE, pH 7.0, without antibiotics and grown to OD₆₀₀ 0.4–0.45. Strains then were diluted 1:10 into THYE buffered to pH 7.0, pH 5.0 or pH 7.0 with 3% (v/v) NaCl and 300 μ l was loaded in triplicate wells on a 100-well Bioscreen C plate and overlaid with mineral oil. Growth was monitored in the Bioscreen C Machine (Growth Curves USA) at 37 °C for 16 h with OD₆₀₀ recorded every 15 min. Doubling times were calculated as described by Khalichi *et al.* (2004). Statistical significance was determined by one-way ANOVA.

ATP hydrolysis activity assay. Permeabilized cells were made essentially as described by Belli & Marquis (1991) using a 25 ml culture of each strain grown to mid-exponential phase (OD₆₀₀ approximately 0.5) in THYE. For assay, 100 μ l permeabilized cells was added to 3 ml assay buffer [50 mM Bistris-HCl (pH 6.0), 10 mM MgCl₂], and the assay was started by adding 3 mM ATP. Reactions were stopped at time points 0, 5 and 10 min by removing an aliquot to iced stop buffer [1.3 parts H₂O, 0.6 parts HCl/molybdate (2.5% w/v NH₄Mo₄O₂·4H₂O, 4.0 M HCl), 0.4 parts 10%, w/v, SDS]. Inorganic phosphate was measured by addition of a 1:10 dilution of Eikonogen (1 M NaHSO₃, 0.1 M Na₂SO₃, 0.01 M 4-amino-3-hydroxyl-1-naphthalenesulfonic acid) followed by a 30 min incubation at room temperature with absorbance read at OD₇₀₀. Assays were performed in quadruplicate. Whole-cell protein concentrations were determined

by BCA assay with BSA standards. Enzyme activity was calculated as $\text{nmol Pi min}^{-1} (\text{mg protein})^{-1}$. Statistical differences were determined using Student's *t*-test.

GAPDH assay of whole cells. Whole cell GAPDH activity was determined using cells grown for 16 h in THYE as described previously (Seifert *et al.*, 2003) with the following modifications. Cells were harvested by centrifugation and suspended to OD_{600} 1.0, in 25 mM Tris-HCl (pH 7.5), 5 mM EDTA. For assay, 1 ml cell suspension was pelleted and resuspended in 900 μl 40 mM triethanolamine, 50 mM Na_2HPO_4 , 5 mM EDTA, pH 8.6, and OD_{600} measured again. For each assay, 7 μl glyceraldehyde-3-phosphate (50 mg ml^{-1} , Sigma) and 100 μl 10 mM NAD^+ were added, and the mixtures were incubated at 37 °C for 30 min. Cells were removed by centrifugation and A_{340} of the supernatants was read and standardized by dividing this value by the measured OD_{600} . Assays were performed in triplicate for each strain. Statistical differences were determined using Student's *t*-test.

Comparison of cell-surface-localized P1 by whole cell dot-blot. Wild-type and YidC mutant strains were compared for their reactivity with a panel of extensively characterized monoclonal antibodies (McArthur *et al.*, 2007) directed against the surface-localized protein adhesin P1 by whole-cell dot-blot as described previously (Seifert *et al.*, 2004) using anti-P1 mAbs 4-10A, 1-6F, 5-5D, 6-11A, 3-10E ascites fluids at a 1:500 dilution.

Evaluation of *S. mutans* adherence by surface plasmon resonance. Adherence of *S. mutans* wild-type and YidC mutant strains to a salivary agglutinin-coated chip surface was evaluated by surface plasmon resonance. Studies were performed on a BIAcoreR 3000 using a Pioneer F1 sensor chip as described previously (Oli *et al.*, 2006).

Biofilm formation and analysis. Formation of wild-type and YidC mutant strain biofilms was assessed as described previously (Hasona *et al.*, 2007). Statistical significance relative to the wild-type value at each time point and growth condition was determined using Student's *t*-test.

Assessment of *S. mutans* colonization and cariogenicity in gnotobiotic rats. *In vivo* colonization and cariogenicity was assessed in gnotobiotic rats using a previously described method (Crowley *et al.*, 1999). Statistical significance in mean caries scores, c.f.u. per mandible and body weights between groups of rats infected with the wild-type strain compared with those infected with the YidC mutant strains was determined by one-way ANOVA with the Tukey-Kramer multiple comparison test using the InStat program (Graphpad Software). Differences between groups were considered significant at a *P*-value <0.05.

RESULTS

Double elimination of *yidC1* and *yidC2* is lethal in *S. mutans*

To enable simultaneous elimination of endogenous YidC1 and YidC2 in *S. mutans*, a conditional expression system was developed for *yidC2*. The *yidC2* gene was fused to the *celB* promoter and placed into the *gtfA* locus of the $\Delta yidC2$ mutant (AH398) chromosome to create strain SP10, where expression of *yidC2* is under the control of the carbon-catabolite-repressible *celB* promoter (Zeng & Burne, 2009). Strain SP20 was produced by replacing *yidC1* in strain SP10 with a spectinomycin marker (see Fig. S1 for schematic). Following growth in different carbohydrates,

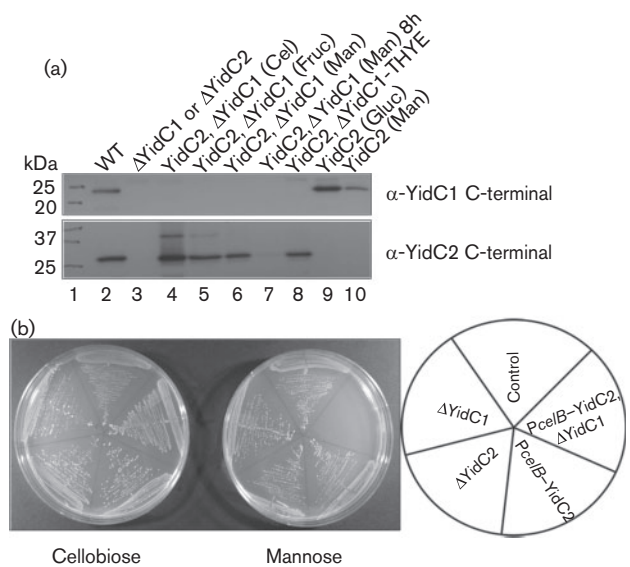


Fig. 1. Western blot of whole-cell lysates of *yidC2* depletion strains (*PcelB*-*yidC2*) SP20 and SP10 grown in various sugars. (a) Lysates were prepared from cultures grown in TDM supplemented with 0.5% of the indicated sugar, reacted with anti-YidC1 C-terminal antibody (top panel) or with anti-YidC2 C-terminal antibody (bottom panel). The wild-type NG8 strain (WT) and AH374 ($\Delta yidC1$) or AH398 ($\Delta yidC2$) mutant strains were used as positive and negative controls, respectively. Cel, cellobiose; Fruc, fructose; Man, mannose; Gluc, glucose. (b) Growth of various strains on TDM 0.5% mannose or 0.5% cellobiose agar plates. The key is shown to the right. Strains used: control (SP22) *NG8 gtfA::em*, $\Delta yidC1$ (AH374), $\Delta yidC2$ (AH398), *PcelB*-YidC2 (SP10), *PcelB*-YidC2, $\Delta yidC1$ (SP20).

YidC2 production was evaluated by Western blot using YidC2 and YidC1 C-terminal antibodies (Fig. 1a). Growth in TDM-cellobiose (inducing sugar) or THYE (rich media) resulted in a high level of YidC2 production (Fig. 1a, lanes 4 and 8, respectively). Growth in TDM-fructose did not repress expression of *yidC2* (Fig. 1a, lane 5); however, growth in TDM-mannose resulted in a substantial decrease of YidC2 after 4 h (lane 6), with near complete repression after 8 h (lane 7). Suppression of YidC2 occurred in the presence of both glucose and mannose in strain SP10 where YidC1 was present (Fig. 1a, lanes 9 and 10). Growth of SP10, SP20 and appropriate control strains was assessed on TDM agar with 0.5% cellobiose or 0.5% mannose (Fig. 1b). Both SP10 and SP20 grew on agar containing cellobiose (*PcelB*-*yidC2*-inducing conditions), while only SP10 grew on agar with mannose (*PcelB*-*yidC2*-repressing conditions). This confirms that double elimination of YidC1 and YidC2 is lethal in *S. mutans*.

The C terminus of YidC2 is important for stress tolerance

YidC1 and YidC2 have approximately 30% sequence identity and approximately 75% similarity. The major

Table 2. Mean generation times of *S. mutans yidC* mutants and complemented strains grown in THYE broth under non-stress, acid-stress and osmotic-stress conditions

Mean generation times (min) \pm SD were calculated based on growth curves completed in triplicate in a Bioscreen C 100-well microtitre plate; OD₆₀₀ was monitored in the Bioscreen C. NG, No growth. Statistical differences compared with: SP22, * P <0.001, ** P <0.05; AH378 † P <0.001, †† P <0.01; AH412 ‡ P <0.01.

Strain	Relevant characteristics	pH 7.0	pH 5.0	3 % NaCl
SP22	NG8 <i>gtfA::em</i>	73 \pm 4.7	167 \pm 6.6†	240 \pm 17.6
SP17	$\Delta yidC2$ <i>gtfA::yidC2</i>	77 \pm 1.5†	285 \pm 4.2*††	334 \pm 27.5
AH378	NG8 $\Delta yidC2::km$	114 \pm 1.7*	346 \pm 19.4*	401 \pm 24.0*
AH374	NG8 $\Delta yidC1::em$	77 \pm 11.9†	186 \pm 5.6†	266 \pm 27.8††
SP13	AH378 <i>gtfA::yidC1C2</i>	80 \pm 1.5†	282 \pm 19.0*††	346 \pm 2.7**
SP14	AH378 <i>gtfA::yidC2C1</i>	171 \pm 5.3*†	390 \pm 41.7*	NG
AH412	NG8 <i>yidC2</i> Δ C:: <i>em</i>	83 \pm 10.0†	367 \pm 0.0*	399 \pm 40.0*
SP16	AH412 $\Delta yidC1::sp$	143 \pm 3.2*†	431 \pm 17.8*†‡	NG

differences are in their C-terminal tails with YidC2's tail being longer and more basic (illustrated in Fig. S2). To investigate the functional difference between the tails, genes encoding chimeric proteins YidC1–C2 and YidC2–C1 were engineered and placed into the *gtfA* locus in the chromosome of a $\Delta yidC2$ mutant to create strains SP13 and SP14 (illustrated in Figs S1 and S2), respectively. Strain SP17 also was generated in which full-length *yidC2* was placed in the *gtfA* locus for use as a control; proper expression was confirmed by Western blot with C-terminal-specific antibodies against YidC1 and YidC2, as well as a non-C-terminal anti-YidC2 antibody (not shown). All strains were tested for the ability to tolerate acid and osmotic stress by growth in THYE broth at pH 5.0 or with 3 % NaCl (pH 7.0) compared with growth under non-stress (pH 7.0) conditions. Mean generation times are shown in Table 2. YidC1–C2 (SP13) was able to restore acid tolerance to the $\Delta yidC2$ mutant to the same level as the positive control SP17 strain. Salt tolerance was also partially restored and similar in strains SP13 and SP17. In contrast with the complementation observed in strain SP13, the growth defect of strain SP14 (expressing YidC2–C1) was significantly worse under non-stress conditions than that of the $\Delta yidC2$ mutant. This shows that substitution of the C terminus of YidC2 with that of YidC1 interferes with normal YidC2 function, resulting perhaps in a non-functional sink for YidC2 substrates. The critical nature of the YidC2 C terminus is also supported by the fact that placing it onto YidC1 (SP13) confers on YidC1–C2 the ability to restore acid tolerance to the $\Delta yidC2$ mutant. The *yidC2* C-terminal deletion strain AH412 showed similar acid and salt sensitivity to the complete *yidC2* deletion strain AH378. Deletion of *yidC1* in the *yidC2* Δ C background (strain SP16) further exacerbated the growth defects of this mutant.

ATPase activity is restored by chimeric YidC1–C2

In *S. mutans* the F₁F₀ ATPase plays a large role in acid tolerance by pumping excess protons out of the cytoplasm.

The mechanisms of insertion of the F₁F₀ ATPase in *S. mutans* membranes are not known; however, mutations of *ffh* or *yidC2* decrease acid tolerance and membrane-associated ATPase activity (Crowley *et al.*, 2004; Hasona *et al.*, 2005). In previous work, a deletion of *yidC1* had no apparent effect on acid tolerance or membrane-associated ATPase activity (Hasona *et al.*, 2005), leading to the hypothesis that, in *S. mutans*, YidC2 and the SRP pathways are involved in the assembly of the F-ATPase, while YidC1 is not. In the current study, ATP hydrolysis activity was evaluated using permeabilized whole cells, as opposed to membranes, prepared by the method of Vadeboncoeur *et al.* (1991) as described previously. As shown in Fig. 2(a), there was a significant decrease in whole-cell ATPase activity in both the $\Delta yidC1$ (AH374) and $\Delta yidC2$ (AH378) mutants compared with the wild-type, albeit more pronounced in the $\Delta yidC2$ mutant. ATPase activity was significantly increased, although not to wild-type levels, by expression of *yidC2* (SP17) or chimeric *yidC1*–C2 (SP13) from the *gtfA* promoter in the $\Delta yidC2$ mutant background. ATPase activity was not complemented in the $\Delta yidC2$ mutant strain expressing the chimeric *yidC2*–C1 gene (SP14).

Extracellular GAPDH activity is increased in *yidC* mutants

GAPDH, as well as a number of other cytoplasmic proteins, has been found on the surface of *S. mutans* and other streptococci (Henderson & Martin, 2011; Ling *et al.*, 2004; Severin *et al.*, 2007). An investigation by Biswas & Biswas (2005) found that deletion of the HtrA extracellular protease/chaperone resulted in increased levels of extracellular GAPDH in culture media. It is not known how GAPDH or other cytoplasmic proteins are transported, as they do not contain signal peptides. To analyse a potential role of YidC1 or YidC2 in GAPDH transport, we tested for differences in cell-surface-localized extracellular GAPDH activity using whole cells. There was a significant increase in extracellular GAPDH activity in the $\Delta yidC2$ mutant

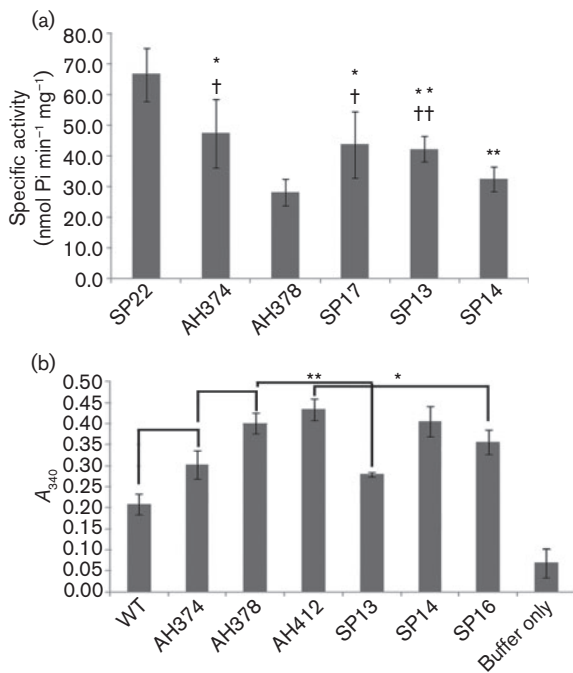


Fig. 2. ATPase and extracellular GAPDH activity of wild-type *S. mutans* and *yidC* mutants. (a) ATPase activity of permeabilized whole cells. Average specific activity is expressed in nmol Pi min⁻¹ mg⁻¹ whole-cell protein. Bars represent mean \pm SD for triplicate assays. Statistically significant differences are indicated, * $P \leq 0.05$ and ** $P \leq 0.01$ compared with SP22, or † $P \leq 0.05$ and †† $P \leq 0.01$ compared with AH378. (b) Extracellular GAPDH activity. Results are expressed as A_{340} , standardized for cell number. Statistically significant differences are indicated, * $P \leq 0.02$, ** $P \leq 0.001$. Descriptions of strains are as follows: WT (wild-type NG8), SP22 (*gtfA::em*), AH374 ($\Delta yidC1$), AH378 ($\Delta yidC2$), AH412 (*yidC2* Δ C), SP13 ($\Delta yidC2$, *gtfA::yidC1-C2*), SP14 ($\Delta yidC2$, *gtfA::yidC2-C1*) and SP16 (*yidC2* Δ C, $\Delta yidC1$).

compared with the $\Delta yidC1$ mutant or wild-type NG8 (Fig. 2b). The *yidC2* Δ C (AH412) strain also demonstrated significantly increased surface-localized GAPDH activity, at a level similar to $\Delta yidC2$ mutant. Expression of *yidC1-C2* (SP13) restored GAPDH activity toward wild-type levels in the $\Delta yidC2$ mutant. Expression of *yidC2-C1* (SP14) did not result in complementation. When *yidC1* was deleted in the *yidC2* Δ C background (SP16), GAPDH activity was significantly decreased compared with the *yidC2* Δ C strain (AH412). Thus, whatever the cause for increased GAPDH activity that occurs in the absence of YidC2's C terminus, the effect can be alleviated to some extent by additionally deleting *yidC1*.

Effects of YidC1 and YidC2 on secreted proteins

The ability of *S. mutans* to form biofilms is dependent on the secretion of extracellular GTFs and FTFs (Banas & Vickerman, 2003) and the cell surface-localized-protein adhesin P1 (antigen I/II, PAc) (Jenkinson & Demuth,

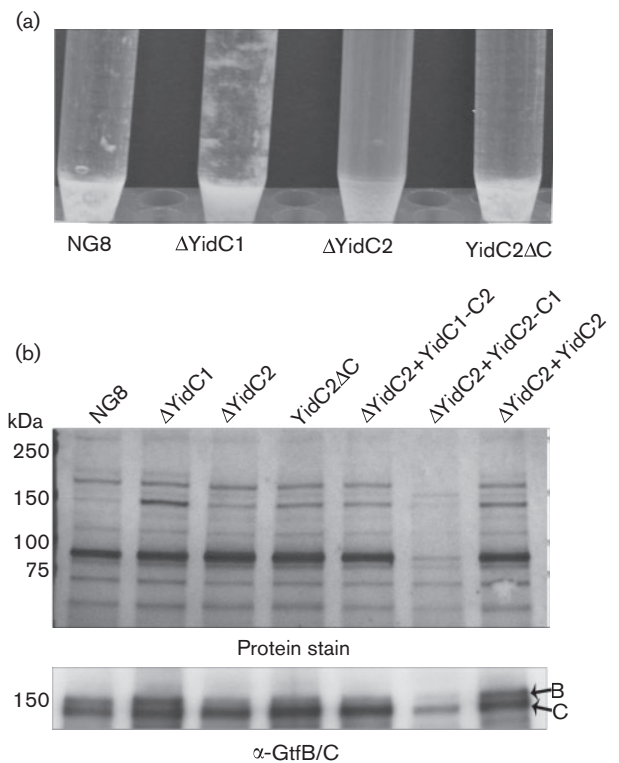


Fig. 3. Cell clumping of stationary-phase cultures and detection of secreted GtfB/GtfC in culture supernatants from *S. mutans* wild-type and *yidC* mutants. (a) Cells were grown in TDM supplemented with 0.5% sucrose for 16 h. (b) Culture supernatants from *S. mutans* cells grown 16 h in THYE were TCA-precipitated and proteins were separated on a 4–15% Bio-Rad TGX gradient gel. The top panel shows the colloidal gold protein stain. The bottom panel shows the Western blot using polyclonal anti-GtfB/C serum.

1997). The $\Delta yidC2$ mutant is impaired in sucrose-dependent biofilm formation and shows decreased clumping in defined media containing 0.5% sucrose compared with wild-type NG8 (Fig. 3a). The *yidC2* Δ C mutant also shows diminished clumping under these conditions. Conversely, the $\Delta yidC1$ mutant displays a hyper-clumping phenotype. The amount of extracellular secreted proteins in culture supernatants of wild-type and mutant strains was evaluated following standardization of bacterial numbers of respective cultures by optical density and is shown in Fig. 3(b) (protein stain). The presence of GtfB and GtfC in the culture supernatants was investigated by Western blot using a polyclonal rabbit antiserum that recognizes both GtfB (162 kDa) and GtfC (160 kDa). A decreased level of GtfB was observed in the $\Delta yidC2$ as well as in the *yidC2* Δ C mutant culture supernatants (Fig. 3b). The level of GtfB was restored in the $\Delta yidC2$ mutant background when *yidC2* was expressed from the *gtfA* promoter ($\Delta yidC2 + YidC2$). Complementation of the $\Delta yidC2$ mutant by chimeric *yidC1-C2* ($\Delta yidC2 + YidC1-C2$) was minimal compared with complementation with the unaltered *yidC2*. When chimeric *yidC2-C1* was

expressed in the $\Delta yidC2$ mutant ($\Delta YidC2 + YidC2-C1$), a more severe dominant-negative phenotype was observed compared with simple deletion of *yidC2*. There was a pronounced decrease in the overall level of secreted proteins detected in the culture supernatant of this strain (Fig. 3b, protein stain), including GtfB and GtfC (Fig. 3b, α -GtfB/C). On the other hand, the $\Delta yidC1$ mutant displayed an overall increase in the level of secreted proteins, particularly GtfB and GtfC, in the culture supernatant compared with the wild-type (protein stain, Fig. 3b). This is consistent with the hyper-clumping seen with this mutant.

When the $\Delta yidC1$, $\Delta yidC2$ and *yidC2* ΔC mutant strains were tested for the presence of surface-localized adhesin P1, results were consistent with those observed with the GTFs, with the exception that eliminating the C terminus of YidC2 had no effect on P1. There was notably more reactivity of a panel of anti-P1 monoclonal antibodies with *S. mutans* whole cells lacking YidC1, but less reactivity with the mutant lacking YidC2, compared with the parent NG8 strain (Fig. 4a). P1 has a highly unusual tertiary structure (Larson *et al.*, 2010) and the binding sites of the mAbs, several of which recognize complex conformational epitopes (McArthur *et al.*, 2007), have now been mapped on the 3D model (Robinette *et al.*, 2011). While there was an overall decrease in immunoreactivity of all anti-P1 antibodies tested in the absence of YidC2, the binding of

some antibodies was affected more than others. mAbs 1-6F and 3-10E were most affected by the deletion, while 4-10A was least affected. This was a consistent finding in multiple experiments. This suggests that the presence of YidC2 affects both the amount and conformation of P1 localized on the cell surface. Results of the immunoassays were mirrored when the adherence of *S. mutans* to P1's physiological binding partner, human salivary agglutinin (SAG), was evaluated by surface plasmon resonance (Fig. 4b). The $\Delta yidC1$ mutant was hyper-adherent, the $\Delta yidC2$ mutant was impaired in P1-mediated adherence and the *yidC2* ΔC mutant was unaffected in its interaction with immobilized SAG. Strain PC3370, which lacks the *spaP* gene encoding P1 (Crowley *et al.*, 1999), was non-adherent. The fact that the $\Delta yidC2$ mutant was so severely impaired in P1-mediated adherence to SAG, despite detection of the adhesin on the cell surface, is consistent with an effect on its conformation and indicates that the P1 present is not functionally active as an adhesin. In contrast, P1-mediated aggregation in the presence of fluid-phase SAG was far less affected and only slightly diminished in the $\Delta yidC1$, $\Delta yidC2$ and *yidC2* ΔC mutant strains (data not shown). The binding of P1 to immobilized versus fluid-phase SAG represents two types of interaction that can be inhibited by different subsets of anti-P1 mAbs (Brady *et al.*, 1992). Therefore, the preservation of *S. mutans* aggregation by fluid-phase SAG supports the conclusion that the functional form of P1 in addition to its total amount was influenced by the elimination of YidC2.

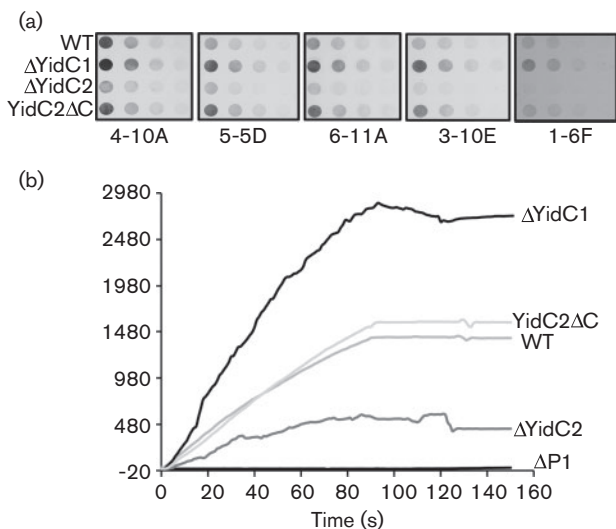


Fig. 4. Anti-P1 mAb reactivity with wild-type (WT) and *yidC* mutant whole cells and comparison of bacterial binding to an agglutinin-coated chip surface. (a) Whole cell dot-blot. Whole bacterial cells serially diluted twofold beginning at 5×10^6 c.f.u. were applied to nitrocellulose membranes and reacted with the anti-P1 mAb indicated below each blot. (b) Surface plasmon resonance (BIAcore) was used to measure adherence of wild-type (WT) and $\Delta YidC$ and $\Delta P1$ mutant cells to a salivary agglutinin-coated chip surface. The sensogram shows the change in resonance units following injection of a suspension of the indicated *S. mutans* background.

Effect of YidC1 and YidC2 on biofilm formation

The contribution of YidC1 and YidC2 to biofilm formation by *S. mutans* was evaluated using hexidium-iodide staining and confocal microscopy (Fig. 5). Biofilm formation under non-stress (pH 7.0) and acid-stress (pH 5.0) conditions was tested using growth in a semi-synthetic medium supplemented with 0.5% sucrose on a glass surface. While growth of the $\Delta yidC1$ mutant is not sensitive to acid (Hasona *et al.*, 2005), biofilm formation by both the $\Delta yidC1$ and $\Delta yidC2$ mutants was notably altered at pH 5.0. The biofilms that did form under this acid-stress condition were too patchy for accurate thicknesses to be measured. Although both were impaired, the biofilm phenotypes of $\Delta yidC1$ and $\Delta yidC2$ mutants differed under non-stress conditions. Elimination of YidC2 resulted in a significantly thinner biofilm at 48 h compared with the wild-type, while elimination of YidC1 did not. Interestingly, biofilm thickness at the earlier 24 h time point was significantly greater in the $\Delta yidC1$ mutant. This is consistent with the increased secretion and cell surface localization of the GtfB/C and P1 proteins that contribute to bacterial adhesion, an early event in biofilm formation.

Effect of YidC1 and YidC2 on *S. mutans* colonization and cariogenicity in rats

A previously described gnotobiotic rat model (Michalek *et al.*, 1975) was used to test the effect of elimination of the

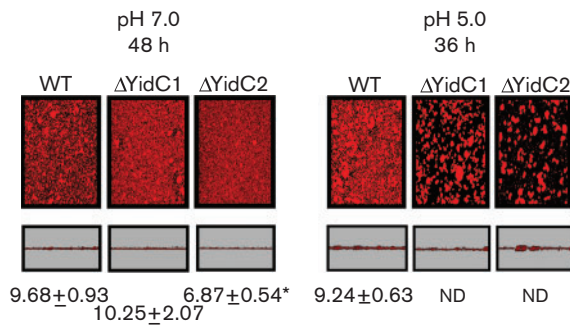


Fig. 5. Biofilm formation by wild-type (WT) and *yidC* mutant strains. Biofilms were allowed to develop for up to 48 h (pH 7.0) or 36 h (pH 5.0) in THYE 0.5% sucrose using hexidium iodide-labelled mid-exponential-phase cultures at the pH conditions indicated. Two areas from each biofilm that formed on the cover glass were visualized and the thicknesses of three sections through each area were measured. Representative images of overhead and side views of biofilms made by each strain are shown. The measured thickness values of biofilm (in μm ; mean \pm SD) of three cross-sections from each of two fields per well performed for duplicate wells are given on the figure. For WT, ΔYidC1 and ΔYidC2 at pH 7.0 after development for 24 h the values were 7.33 ± 0.50 , $8.75 \pm 0.89^*$ and $6.14 \pm 0.71^*$, respectively (significance given below). Each experiment was performed twice. Statistically significant differences compared with the wild-type are indicated. $*P \leq 0.001$. ND, not determined, growth was too patchy to accurately measure thickness.

YidC proteins of *S. mutans* on bacterial colonization and cariogenicity *in vivo* (see Table 3). Statistically significant differences were observed in the sulcal and proximal surface caries scores of animals infected with the ΔyidC1 , ΔyidC2 and $\text{yidC2}\Delta\text{C}$ mutants compared with the NG8 parent strain. In addition, there were significantly fewer buccal caries in animals infected with the ΔyidC2 mutant. Animals from all of the experimental groups were colonized with *S. mutans* at the time they were killed for caries evaluation, 6 weeks post-infection, indicating that the differences in caries scores stemmed from a difference in virulence of the test strains, rather than a simple impairment in their ability to colonize. Interestingly, animals in the ΔyidC1 mutant group, in which there were significantly decreased caries scores, also had a significantly higher degree of colonization at the 6 week time point compared with the other groups.

DISCUSSION

Streptococci have several redundant pathways for protein translocation and secretion, making it difficult to evaluate functions of individual proteins. There are two YidC homologues, including one (YidC2) that may overlap functionally with the SRP to facilitate co-translational translocation (Funes *et al.*, 2009). In this study, a conditional expression system to allow controlled expression of *S.*

Table 3. Colonization and cariogenicity of *S. mutans* wild-type and YidC deletion mutants in gnotobiotic rats

$n=5$ per group. Weights (g): Group A, 162 ± 11 ; Group B, 149 ± 11 ; Group C, 152 ± 8 ; Group D, 145 ± 11.4 . There were no significant differences between the weight of any of the groups. Carious lesion location and severity: E, enamel; Ds, slight dental; Dm, moderate dental; Dx, extensive dental. Significant difference in mean caries score compared with the wild-type strain at each location: $*P < 0.01$, $**P < 0.05$, $***P < 0.001$.

Group (strain)	Mean caries score												$10^{-6} \times \text{c.f.u. per mandible}$
	Buccal						Sulcal						
	E	Ds	Dm	Dx	E	Ds	Dm	Dx	E	Ds	Dm	Dx	
A (wild-type)	13.8 ± 0.4	11.4 ± 0.4	6.2 ± 0.4	3.8 ± 0.6	19.8 ± 0.7	15.8 ± 0.7	7.8 ± 0.9	2.6 ± 0.7	7.2 ± 0.5	4.4 ± 0.4	0.0 ± 0.0	0.0 ± 0.0	11.8 ± 1.5
B (ΔYidC1)	12.8 ± 0.9	9.4 ± 0.8	6.4 ± 0.7	5.4 ± 0.7	$17.0 \pm 0.4^{***}$	$12.0 \pm 0.9^{**}$	6.0 ± 0.4	2.0 ± 0.8	$4.0 \pm 0.0^{**}$	$2.2 \pm 0.9^{**}$	0.2 ± 0.2	0.0 ± 0.0	$23.1 \pm 2.7^{***}$
C (ΔYidC2)	$9.8 \pm 1.0^*$	$6.8 \pm 0.9^*$	4.6 ± 0.7	3.4 ± 0.7	$16.2 \pm 0.2^{***}$	$9.8 \pm 0.7^{***}$	5.4 ± 0.8	1.4 ± 0.5	4.8 ± 0.8	$0.4 \pm 0.4^{***}$	0.0 ± 0.0	0.0 ± 0.0	13.8 ± 0.7
D ($\text{YidC2}\Delta\text{C}$)	10.8 ± 0.4	$7.6 \pm 0.4^{**}$	6.0 ± 0.3	3.8 ± 0.6	$15.6 \pm 0.5^{**}$	$10.4 \pm 0.7^*$	5.6 ± 0.9	1.2 ± 0.5	4.8 ± 0.5	$0.0 \pm 0.0^{***}$	0.0 ± 0.0	0.0 ± 0.0	8.4 ± 1.3

mutans yidC2 upon deletion of *yidC1* revealed that double deletion of YidC1 and YidC2 is lethal in this organism.

A number of strains were constructed to investigate functional differences between the two *S. mutans* YidC proteins and evaluated for growth under no stress, acid-stress and osmotic-stress conditions, as well as for whole-cell ATPase activity, a determinant for acid tolerance (Belli & Marquis, 1991). Results indicated a clear role of the C terminus of YidC2 in stress tolerance. When the C-terminal tail of YidC2 was deleted, bacteria exposed to acid or osmotic stress were similarly impaired for growth and ATPase activity (Funes *et al.*, 2009) compared with those with a complete deletion of *yidC2*. On the other hand, when transformation efficiency was evaluated, deletion of its C terminus had less of an effect compared with elimination of YidC2 in its entirety. Complementation experiments with the yeast mitochondrial homologues Oxa1 and Cox18 have suggested that *S. mutans* YidC2 functions in at least two pathways, and that there are distinct functions of YidC2 that do and do not depend on an intact C terminus (Funes *et al.*, 2009). An intermediate growth phenotype was seen in the *yidC2ΔC* partial mutant under non-stress conditions. Chimeric YidC1–C2 restored stress tolerance and ATPase activity to the *ΔyidC2* mutant, while YidC2–C1 slowed growth even further compared with the un-complemented *ΔyidC2* mutant. YidC2–C1 was unable to complement ATPase activity in the *ΔyidC2* mutant, and this strain displayed a more pronounced defect in secretion with very little protein found in the culture supernatants. Hence, it is likely that the chimeric YidC2–C1 is non-functional and acts as a sink for YidC2 and possibly YidC1 substrates. Taken together, our results indicate that the C terminus is integral to each YidC protein's individual function. Also of note is that in strain SP17, where *yidC2* was expressed from the *gfa* promoter, growth to wild-type levels under stress conditions and ATPase activity were not fully restored. This suggests that the *yidC2* promoter and consequent level of *yidC2* expression also contributes to stress tolerance. In studies of the LiaSR two-component system, *yidC2* expression was upregulated in response to membrane stress through the LiaR response regulator (Suntharalingam *et al.*, 2009). Despite the ability of chimeric YidC1–C2 to complement the *ΔyidC2* mutant strain, knockout of the *yidC1* gene in this background was not possible. It appears therefore that the overall level of YidC expression is important and use of the *yidC2* promoter to express YidC1–C2 may have resulted in full complementation.

A study by Biswas & Biswas (2005) investigated the effects of deletion of the HtrA extracellular protease/chaperone and found that levels of extracellular GAPDH in culture media increased when HtrA was absent. Extracellular GAPDH activity was increased in both *ΔyidC1* and *ΔyidC2* mutants compared with the parental strain, with a greater effect seen with *ΔyidC2*. The *yidC2ΔC* mutant displayed GAPDH activity similar to the *ΔyidC2* mutant. The YidC1–C2 protein was able to partially restore

GAPDH activity toward wild-type levels in the *ΔyidC2* mutant, indicating that the C-terminal tail is important for this YidC function but that this is not the whole story. It is possible that YidC1 and YidC2 are involved in the localization of HtrA. In that case, one would expect their disruption to have a similar effect on extracellular GAPDH to deletion of HtrA.

Cell surface localization of the adhesin P1 was negatively affected by deletion of *yidC2*, as shown by decreased immunoreactivity of anti-P1 antibodies with the *ΔyidC2* strain. Conversely, elimination of *yidC1* resulted in increased detection of P1 on the cell surface. This implies a balanced surface biogenesis mechanism that involves both YidC1 and YidC2, although it is unclear whether the increased immunodetection of P1 on the surface of the *ΔyidC1* mutant reflects an increased abundance of P1 or a decrease in another surface component that allows improved exposure to the antibodies. The respective changes in anti-P1 antibody reactivity in the *ΔyidC1* and *ΔyidC2* mutant strains were associated with corresponding functional differences in P1-mediated adherence determined using surface plasmon resonance. There were similar effects on the levels of extracellular GtfB and GtfC detected in culture supernatants of the *yidC* mutants compared with the wild-type, with a decrease seen in the *ΔyidC2* mutant and an increase in the *ΔyidC1* mutant. The increased secretion of GtfB and GtfC in the *ΔyidC1* mutant suggests that the increased immunodetection of P1 on the cell surface of this strain stems from a real increase in the amount of cell-surface-localized protein secreted rather than an effect on antibody accessibility.

The increase in colonization of rats with the *ΔyidC1* strain compared with the wild-type is consistent with an increase in secretion of the GTFs and the P1 adhesin. The more rapid biofilm formation of the *ΔyidC1* mutant under non-stress conditions is not surprising in light of these findings. Virulence of both the *ΔyidC1* and *ΔyidC2* mutants was negatively affected in these strains as evidenced by decreases in caries scores in rats and aberrant biofilm formation of the *ΔyidC2* mutant under all conditions tested, and the *ΔyidC1* mutant under acid stress at pH 5.0. While the *ΔyidC2* mutant displays a growth defect under both non-stress and acid-stress conditions, the *ΔyidC1* mutant does not (Hasona *et al.*, 2005). Thus the pH 5.0 biofilm phenotype does not appear to stem from poor growth or acid sensitivity, but from another mechanism.

The findings that *S. mutans* YidC1 and YidC2 both contribute to pathways mediating cell surface biogenesis and secretion of extracellular proteins as well as the cellular response to stress furthers our understanding of the complex series of events involved in *S. mutans* pathogenesis, beginning with bacterial adhesion and colonization, and ending with the generation of acid end products and resilience in the face of environmental stress. Taken together, these results suggest that while YidC2 appears to play a more critical role in stress tolerance of *S. mutans*, YidC1 also

contributes to its biology. YidC1 and YidC2 display unique functions and cooperate in an integrated balanced manner in protein secretion and cell wall biogenesis, thus providing an explanation for the inability to simultaneously eliminate both paralogues in this species.

ACKNOWLEDGEMENTS

We would like to thank Drs Lin Zeng and R. A. Burne (University of Florida) for advice in the development of a conditional expression system in *S. mutans* and for the gift of plasmids pBGK2 and pBGE. We would also like to acknowledge Dr Nathan Lewis (University of Florida) for his critical reading of the manuscript. This work was supported by the National Institute of Dental and Craniofacial Research grants F31 DE019605, R01 DE08007 and R01 DE09081

REFERENCES

- Banas, J. A. & Vickerman, M. M. (2003). Glucan-binding proteins of the oral streptococci. *Crit Rev Oral Biol Med* **14**, 89–99.
- Belli, W. A. & Marquis, R. E. (1991). Adaptation of *Streptococcus mutans* and *Enterococcus hirae* to acid stress in continuous culture. *Appl Environ Microbiol* **57**, 1134–1138.
- Biswas, S. & Biswas, I. (2005). Role of HtrA in surface protein expression and biofilm formation by *Streptococcus mutans*. *Infect Immun* **73**, 6923–6934.
- Bonnefoy, N., Fiumera, H. L., Dujardin, G. & Fox, T. D. (2009). Roles of Oxa1-related inner-membrane translocases in assembly of respiratory chain complexes. *Biochim Biophys Acta* **1793**, 60–70.
- Brady, L. J., Piacentini, D. A., Crowley, P. J., Oyston, P. C. & Bleiweis, A. S. (1992). Differentiation of salivary agglutinin-mediated adherence and aggregation of mutans streptococci by use of monoclonal antibodies against the major surface adhesin P1. *Infect Immun* **60**, 1008–1017.
- Buckley, N. D., Lee, L. N. & LeBlanc, D. J. (1995). Use of a novel mobilizable vector to inactivate the *scrA* gene of *Streptococcus sobrinus* by allelic replacement. *J Bacteriol* **177**, 5028–5034.
- Crowley, P. J., Brady, L. J., Michalek, S. M. & Bleiweis, A. S. (1999). Virulence of a *spaP* mutant of *Streptococcus mutans* in a gnotobiotic rat model. *Infect Immun* **67**, 1201–1206.
- Crowley, P. J., Svensäter, G., Snoep, J. L., Bleiweis, A. S. & Brady, L. J. (2004). An *ffh* mutant of *Streptococcus mutans* is viable and able to physiologically adapt to low pH in continuous culture. *FEMS Microbiol Lett* **234**, 315–324.
- Dong, Y., Palmer, S. R., Hasona, A., Nagamori, S., Kaback, H. R., Dalbey, R. E. & Brady, L. J. (2008). Functional overlap but lack of complete cross-complementation of *Streptococcus mutans* and *Escherichia coli* YidC orthologs. *J Bacteriol* **190**, 2458–2469.
- Funes, S., Hasona, A., Bauerschmitt, H., Grubbauer, C., Kauff, F., Collins, R., Crowley, P. J., Palmer, S. R., Brady, L. J. & Herrmann, J. M. (2009). Independent gene duplications of the YidC/Oxa/Alb3 family enabled a specialized cotranslational function. *Proc Natl Acad Sci U S A* **106**, 6656–6661.
- Gibbons, R. J., Cohen, L. & Hay, D. I. (1986). Strains of *Streptococcus mutans* and *Streptococcus sobrinus* attach to different pellicle receptors. *Infect Immun* **52**, 555–561.
- Gutierrez, J. A., Crowley, P. J., Brown, D. P., Hillman, J. D., Youngman, P. & Bleiweis, A. S. (1996). Insertional mutagenesis and recovery of interrupted genes of *Streptococcus mutans* by using transposon Tn917: preliminary characterization of mutants displaying acid sensitivity and nutritional requirements. *J Bacteriol* **178**, 4166–4175.
- Hamilton, I. R. & Buckley, N. D. (1991). Adaptation by *Streptococcus mutans* to acid tolerance. *Oral Microbiol Immunol* **6**, 65–71.
- Hasona, A., Crowley, P. J., Levesque, C. M., Mair, R. W., Cvitkovitch, D. G., Bleiweis, A. S. & Brady, L. J. (2005). Streptococcal viability and diminished stress tolerance in mutants lacking the signal recognition particle pathway or YidC2. *Proc Natl Acad Sci U S A* **102**, 17466–17471.
- Hasona, A., Zuobi-Hasona, K., Crowley, P. J., Abranches, J., Ruelf, M. A., Bleiweis, A. S. & Brady, L. J. (2007). Membrane composition changes and physiological adaptation by *Streptococcus mutans* signal recognition particle pathway mutants. *J Bacteriol* **189**, 1219–1230.
- Heckman, K. L. & Pease, L. R. (2007). Gene splicing and mutagenesis by PCR-driven overlap extension. *Nat Protoc* **2**, 924–932.
- Henderson, B. & Martin, A. (2011). Bacterial virulence in the moonlight: multitasking bacterial moonlighting proteins are virulence determinants in infectious disease. *Infect Immun* **79**, 3476–3491.
- Honda, K., Nakamura, K., Nishiguchi, M. & Yamane, K. (1993). Cloning and characterization of a *Bacillus subtilis* gene encoding a homolog of the 54-kilodalton subunit of mammalian signal recognition particle and *Escherichia coli* Ffh. *J Bacteriol* **175**, 4885–4894.
- Jenkinson, H. F. & Demuth, D. R. (1997). Structure, function and immunogenicity of streptococcal antigen I/II polypeptides. *Mol Microbiol* **23**, 183–190.
- Jenkinson, H. F. & Lamont, R. J. (1997). Streptococcal adhesion and colonization. *Crit Rev Oral Biol Med* **8**, 175–200.
- Khalichi, P., Cvitkovitch, D. G. & Santerre, J. P. (2004). Effect of composite resin biodegradation products on oral streptococcal growth. *Biomaterials* **25**, 5467–5472.
- Kiefer, D. & Kuhn, A. (2007). YidC as an essential and multifunctional component in membrane protein assembly. *Int Rev Cytol* **259**, 113–138.
- Knox, K. W., Hardy, L. N. & Wicken, A. J. (1986). Comparative studies on the protein profiles and hydrophobicity of strains of *Streptococcus mutans* serotype *c*. *J Gen Microbiol* **132**, 2541–2548.
- Larson, M. R., Rajashankar, K. R., Patel, M. H., Robinette, R. A., Crowley, P. J., Michalek, S., Brady, L. J. & Deivanayagam, C. (2010). Elongated fibrillar structure of a streptococcal adhesin assembled by the high-affinity association of α - and PPII-helices. *Proc Natl Acad Sci U S A* **107**, 5983–5988.
- LeBlanc, D. J., Lee, L. N. & Abu-Al-Jaibat, A. (1992). Molecular, genetic, and functional analysis of the basic replicon of pVA380-1, a plasmid of oral streptococcal origin. *Plasmid* **28**, 130–145.
- Ling, E., Feldman, G., Portnoi, M., Dagan, R., Overweg, K., Mulholland, F., Chalifa-Caspi, V., Wells, J. & Mizrahi-Nebenzahl, Y. (2004). Glycolytic enzymes associated with the cell surface of *Streptococcus pneumoniae* are antigenic in humans and elicit protective immune responses in the mouse. *Clin Exp Immunol* **138**, 290–298.
- McArthur, W. P., Rhodin, N. R., Seifert, T. B., Oli, M. W., Robinette, R. A., Demuth, D. R. & Brady, L. J. (2007). Characterization of epitopes recognized by anti-*Streptococcus mutans* P1 monoclonal antibodies. *FEMS Immunol Med Microbiol* **50**, 342–353.
- Michalek, S. M., McGhee, J. R. & Navia, J. M. (1975). Virulence of *Streptococcus mutans*: a sensitive method for evaluating cariogenicity in young gnotobiotic rats. *Infect Immun* **12**, 69–75.
- Oli, M. W., McArthur, W. P. & Brady, L. J. (2006). A whole cell BIAcore assay to evaluate P1-mediated adherence of *Streptococcus mutans* to human salivary agglutinin and inhibition by specific antibodies. *J Microbiol Methods* **65**, 503–511.

- Phillips, G. J. & Silhavy, T. J. (1992).** The *E. coli* *ffh* gene is necessary for viability and efficient protein export. *Nature* **359**, 744–746.
- Robinette, R. A., Oli, M. W., McArthur, W. P. & Brady, L. J. (2011).** A therapeutic anti-*Streptococcus mutans* monoclonal antibody used in human passive protection trials influences the adaptive immune response. *Vaccine* **29**, 6292–6300.
- Seifert, K. N., McArthur, W. P., Bleiweis, A. S. & Brady, L. J. (2003).** Characterization of group B streptococcal glyceraldehyde-3-phosphate dehydrogenase: surface localization, enzymatic activity, and protein–protein interactions. *Can J Microbiol* **49**, 350–356.
- Seifert, T. B., Bleiweis, A. S. & Brady, L. J. (2004).** Contribution of the alanine-rich region of *Streptococcus mutans* P1 to antigenicity, surface expression, and interaction with the proline-rich repeat domain. *Infect Immun* **72**, 4699–4706.
- Severin, A., Nickbarg, E., Wooters, J., Quazi, S. A., Matsuka, Y. V., Murphy, E., Moutsatsos, I. K., Zagursky, R. J. & Olmsted, S. B. (2007).** Proteomic analysis and identification of *Streptococcus pyogenes* surface-associated proteins. *J Bacteriol* **189**, 1514–1522.
- Suntharalingam, P., Senadheera, M. D., Mair, R. W., Lévesque, C. M. & Cvitkovitch, D. G. (2009).** The LiaFSR system regulates the cell envelope stress response in *Streptococcus mutans*. *J Bacteriol* **191**, 2973–2984.
- Terleckyj, B., Willett, N. P. & Shockman, G. D. (1975).** Growth of several cariogenic strains of oral streptococci in a chemically defined medium. *Infect Immun* **11**, 649–655.
- Vadeboncoeur, C., Brochu, D. & Reizer, J. (1991).** Quantitative determination of the intracellular concentration of the various forms of HPr, a phosphocarrier protein of the phosphoenolpyruvate: sugar phosphotransferase system in growing cells of oral streptococci. *Anal Biochem* **196**, 24–30.
- van der Laan, M., Urbanus, M. L., Ten Hagen-Jongman, C. M., Nouwen, N., Oudega, B., Harms, N., Driessen, A. J. & Luirink, J. (2003).** A conserved function of YidC in the biogenesis of respiratory chain complexes. *Proc Natl Acad Sci U S A* **100**, 5801–5806.
- Wen, Z. T. & Burne, R. A. (2001).** Construction of a new integration vector for use in *Streptococcus mutans*. *Plasmid* **45**, 31–36.
- Wunder, D. & Bowen, W. H. (2000).** Effects of antibodies to glucosyltransferase on soluble and insolubilized enzymes. *Oral Dis* **6**, 289–296.
- Zeng, L. & Burne, R. A. (2009).** Transcriptional regulation of the cellobiose operon of *Streptococcus mutans*. *J Bacteriol* **191**, 2153–2162.
- Zhang, Y. J., Tian, H. F. & Wen, J. F. (2009).** The evolution of YidC/Oxa/Alb3 family in the three domains of life: a phylogenomic analysis. *BMC Evol Biol* **9**, 137.

Edited by: D. Demuth